

1 **Regional-scale jet waviness modulates the occurrence of**
2 **mid-latitude weather extremes**

3 **Matthias Röthlisberger¹, Stephan Pfahl² and Olivia Martius^{1,3}**

4 ¹Oeschger Centre for Climate Change Research and Institute of Geography, University of Bern, Bern, Switzerland

5 ²Institute for Atmospheric and Climate Science, ETH Zürich, Zürich, Switzerland

6 ³Mobilair Lab for Natural Risks, University of Bern, Bern, Switzerland

7 **Key Points:**

- 8 • Regional-scale jet waviness significantly modulates the number and location of weather
9 extremes
- 10 • Weather extremes are primarily affected by regional-scale rather than hemispheric jet
11 waviness
- 12 • The strength and sign of the waviness-extremes link differs between regions

Corresponding author: Matthias Röthlisberger, matthias.roethlisberger@giub.unibe.ch

Abstract

Several studies have attributed the occurrence of recent weather extremes to an amplified waviness of the upper-tropospheric jet stream. Although trends in jet waviness are still under discussion, it is crucial to better understand the mechanisms through which jet waviness affects weather extremes. Here we show that variations in jet waviness on regional scales effectively modulate the occurrence of daily weather extremes, however, in regionally different ways. The jet waviness over the North Atlantic and the North Pacific mainly affects where wind, precipitation and cold extremes occur, while a wavy jet over Eurasia strongly favors the occurrence of hot extremes in summer. This is because regional variations of jet waviness are intrinsically linked to the occurrence and tracks of synoptic-scale weather systems, which can trigger the extremes. We conclude that potential jet waviness changes would affect the occurrence of weather extremes differently depending on where these changes occur.

1 Introduction

In recent years the Northern Hemisphere mid-latitudes have been hit by a remarkable series of high-impact weather extremes including the record breaking heat waves in Europe in 2003 [Black *et al.*, 2004] and in Russia in 2010 [Barriopedro *et al.*, 2011], severe floods in the United Kingdom in 2013/2014 [Herring *et al.*, 2014] and unusually cold winters with devastating winter storms in the eastern United States [Palmer, 2014; Vose *et al.*, 2014]. The number, diversity and severity of these weather extremes has triggered an engaged debate on the causes of their temporally clustered occurrence. While a change in the frequency of some extremes is expected with global warming [IPCC, 2012; Coumou and Rahmstorf, 2012; Schneider *et al.*, 2015; Hoskins and Woollings, 2015], most studies agree that the recent series of mid-latitude weather extremes cannot be explained by the observed shift in the mean temperature and thermodynamic arguments alone [Horton *et al.*, 2015]. Hence, these weather extremes must at least partly be related to anomalous atmospheric circulation patterns [Horton *et al.*, 2015; Hoskins and Woollings, 2015].

Several studies have proposed that increased waviness of the polar jet has favored the occurrence of particular weather extremes [Francis and Vavrus, 2012; Petoukhov *et al.*, 2013; Screen and Simmonds, 2014; Francis and Vavrus, 2015; Francis and Skific, 2015]. Previous studies investigating this “waviness-extremes” link have mainly focused on long-lasting extremes on continental to hemispheric scales [Liu *et al.*, 2012; Petoukhov *et al.*, 2013; Coumou *et al.*, 2014; Screen and Simmonds, 2014]. Statistically significant links between jet waviness on a

45 hemispheric scale and monthly temperature and precipitation extremes could be established
46 for several mid-latitude regions [Screen and Simmonds, 2014]. On synoptic (multi-day) time-
47 scales, periods of frequently occurring temperature and precipitation extremes have recently
48 been linked to low- and high storm track activity, respectively [Lehmann and Coumou, 2015;
49 Coumou et al., 2015]. However, one particularly important aspect of this topic has not been
50 investigate so far, namely regional variations in the strength and sign of this link.

51 A variety of jet waviness measures have been proposed in recent studies. Some of them
52 conceptualize jet waviness as the amplitudes of the excursions of geopotential height isopleths
53 or isentropic PV contours from a zonal background state [Francis and Vavrus, 2012, 2015; Screen
54 and Simmonds, 2013a; Röthlisberger et al., 2016]. Others rely on Fourier analysis of the merid-
55 ional wind or the geopotential height in particular latitude bands [Petoukhov et al., 2013; Coumou
56 et al., 2014; Screen and Simmonds, 2013a, 2014] as an indication for wave amplitudes. The
57 use of these conceptually different types of waviness measures may lead to contradicting re-
58 sults, as a number of studies has shown that trends in jet waviness as inferred from these dif-
59 ferent measures do not generally agree [Barnes, 2013; Barnes and Screen, 2015; Screen and
60 Simmonds, 2013b].

61 Here, we use the regional-scale jet waviness measure introduced by Röthlisberger et al.
62 [2016] only to discriminate between regionally wavy and zonal upper-level flow configurations
63 and investigate, where and how a regionally wavy (or zonal) jet favors or hampers the occur-
64 rence of daily weather extremes.

65 It is well established that mid-latitude weather extremes often occur in association with
66 synoptic-scale weather systems such as cyclones and blocking anticyclones and that these weather
67 systems are steered by the upper-level flow [e.g., Dickson and Namias, 1976; Davies, 2015].
68 For example precipitation and wind extremes in winter occur preferentially in or near extra-
69 tropical cyclones [Donat et al., 2010; Pfahl and Wernli, 2012a; Vose et al., 2014]. Winter cold
70 extremes in western Europe and the Mediterranean often occur during cold air outbreaks down-
71 stream of North Atlantic blocking [Sillmann et al., 2011; Buehler et al., 2011] and in the same
72 way blocking over the North Pacific favors cold extremes in western North America [Whan
73 et al., 2016]. Summer heat extremes, in contrast, tend to occur near the center of blocking an-
74 ticyclones [Pfahl and Wernli, 2012b], mainly for two reasons: Firstly, subsiding air within the
75 blocks and the resulting clear sky conditions lead to increased solar irradiation reaching the
76 Earth's surface [Black et al., 2004; Barriopedro et al., 2011; Pfahl and Wernli, 2012b]. Sec-

77 only, the adiabatic warming of the subsiding air leads to reduced relative humidity and pre-
78 vents precipitation. The lack of precipitation as well as the increased solar irradiation both con-
79 tribute to soil moisture depletion which in turn increases the surface sensible heat flux [e.g.,
80 *Namias, 1960; Fischer et al., 2007; Seneviratne et al., 2010*]. Over the oceans the influence of
81 blocking on extreme temperature is much reduced, on the one hand due to the larger heat ca-
82 pacity compared to the land surface (and hence less temperature variability on synoptic time
83 scales) but also due to the lack of the soil-moisture coupling [*Pfahl and Wernli, 2012b*].

84 From a meteorological point of view it is therefore clear that weather systems are cru-
85 cial for understanding the waviness-extremes link. However, in the recent literature their piv-
86 otal role in linking the upper-level flow to surface weather extremes has not been considered
87 sufficiently. In this study we thus aim to contribute to this current discussion in two ways: Firstly,
88 we analyze this waviness-extremes link regionally and show that the strength and sign of this
89 link varies between regions and types of extremes. Secondly, we use feature based climatolo-
90 gies of extratropical cyclones and blocking anticyclones to illustrate the regionally varying role
91 of weather systems in linking jet waviness to the occurrence of surface weather extremes.

92 **2 Data and Methods**

93 **2.1 Extremes and Jet Waviness Data**

94 The ERA-Interim re-analysis data set [*Dee et al., 2011*] (interpolated to $1^\circ \times 1^\circ$ hori-
95 zontal resolution, covering the period of 1979-2012) is used to identify daily extremes of daily
96 maximum 10 m wind gusts (ERA-Interim variable "10 metre wind gust since previous post-
97 processing"), daily maximum 2 m temperature, daily minimum 2 m temperature and daily ac-
98 cumulated precipitation as the 5% most extreme values per season at every grid point. These
99 data stem from short term model predictions (with lead times between 6 and 18 h) of the Eu-
100 ropean Centre for Medium-Range Weather Forecasts (ECMWF) Integrated Forecast System
101 (IFS) model which was used for producing the ERA-Interim data set. Note that the absolute
102 values of the extremes are largely irrelevant for our analysis. Rather it is the timing of the ex-
103 treme events that matters for this analysis and previous studies have reported that in the ex-
104 tratropics this timing is reasonably well represented in ERA-Interim [*Pfahl and Wernli, 2012a*].

105 The waviness of the polar jet is measured separately in the Eurasian (0°E - 135°E), North
106 Pacific (135°E - 120°W), North American (120°W - 60°W) and North Atlantic (60°W - 0°E)
107 sectors using the jet waviness measure introduced by *Röthlisberger et al.* [2016]. This wavi-

ness measure is based on isentropic potential vorticity (PV) fields from ERA-Interim (on the 320 K isentrope in winter and on 335 K in summer), and uses the geometry of the 2 potential vorticity unit (PVU) contours on these isentropes as an indicator for the waviness of the polar jet. The 2 PVU contour (i.e., the dynamical tropopause) on these isentropes is co-located with the polar jet and hence the contour geometry is an excellent indicator for the waviness of the polar jet. The jet waviness of a particular longitudinal sector is calculated by integrating absolute values of latitude changes of the 2 PVU contour along this contour over the length of the sector. High waviness results from large-amplitude meridional meanders of the polar jet, while low waviness is obtained for zonally orientated jet segments. The waviness values are calculated from 6-hourly PV fields and then averaged to obtain daily waviness time series covering the period 1979-2012 for all sectors. High (low) waviness days for a particular sector are defined as days on which the respective waviness value falls into the highest (lowest) quartile of the waviness distribution of the respective season and sector. The technical details of the waviness measure are described in Supporting Text S1 [Martius *et al.*, 2010].

2.2 Odds Ratios

Using these extremes and jet waviness data, the odds ratio (OR) of the occurrence of an extreme during high (low) waviness in a particular sector is calculated at each grid point as

$$\text{OR} = \frac{P(\text{Ext}|\text{Wave})(1 - P(\text{Ext}))}{P(\text{Ext})(1 - P(\text{Ext}|\text{Wave}))} \quad (1)$$

where $P(\text{Ext}|\text{Wave})$ is the probability of observing an extreme at the respective grid point during a day with high (low) waviness, estimated as the number of high (low) waviness days with a co-occurring extreme divided by the total number of high (low) waviness days. $P(\text{Ext})$ is the probability of observing an extreme at any day, i.e., 0.05. With this approach we thus assess, how frequently weather extremes co-occur with a regionally wavy (or zonal) jet compared to their climatological frequency (see Stephenson [2000] and Chapter 8.2.2 in Wilks [2011] for a discussion of the use of odds ratios in atmospheric sciences).

The significance of the ORs is assessed in a two step approach. First, a Monte-Carlo method is applied to estimate p -values of the ORs at each grid point. Random waviness time series are constructed for each region and season by shuffling the 34 seasons of the original time series and connecting these shuffled seasons to a random 34-season waviness time series. This

137 shuffling of entire seasons is necessary, as for some sectors, the original waviness time series
138 exhibit substantial sub-seasonal variability, which, if not taken into account, strongly affects
139 the resulting p -values. By shuffling entire seasons, however, we ensure that the random time
140 series retain the autocorrelation and sub-seasonal variability of the original waviness data. This
141 procedure is repeated 1000 times, and p -values at each grid point are estimated through com-
142 parison with the distribution of ORs from these samples. In a second step, the False Discov-
143 ery Rate (FDR) test by *Benjamini and Hochberg* [1995] is applied to the entire set of p -values
144 from a given OR field. This test controls the number of falsely rejected null hypotheses in mul-
145 tiple statistical testing. A maximum false discovery rate of 5% is chosen here. Note that, while
146 this test was originally developed for independent data, *Ventura et al.* [2004] have shown that
147 it also correctly controls the number of falsely rejected hypotheses in applications with spa-
148 tially correlated climatological data.

149 **2.3 Blocking and Extratropical Cyclone Climatologies**

150 To interpret the OR fields we incorporate objective climatologies of atmospheric block-
151 ing and extratropical cyclones into our analysis. We use the algorithm developed by *Schwierz*
152 *et al.* [2004] to compile a climatology of atmospheric blocking and an updated version of the
153 cyclone climatology of *Wernli and Schwierz* [2006] (see Supporting Texts S2 and S3 for de-
154 scriptions of the identification algorithms). The seasonal climatologies of atmospheric block-
155 ing and extratropical cyclones are shown in Supporting Figure 1.

156 **3 Results and Discussion**

157 **3.1 Spatially Aggregated Effect of Regional-Scale and Hemispheric Jet Waviness on** 158 **Weather Extremes**

159 We first discuss the effect of linking regional-scale rather than hemispheric jet waviness
160 with the extremes. Previous studies found that prolonged weather extremes, especially over
161 land areas, occur more frequently during periods with high jet waviness on a hemispheric scale
162 [*Liu et al.*, 2012; *Petoukhov et al.*, 2013; *Coumou et al.*, 2014; *Screen and Simmonds*, 2014].
163 Here we investigate, whether high regional-scale jet waviness is also consistently linked to more
164 extremes. Figure 1 depicts the size of the northern hemisphere land area with significant ORs
165 for high waviness and all four types of extremes. For high waviness, the majority of the sig-
166 nificant ORs is larger than one, while the opposite is true for low jet waviness (Supporting Fig-

167 ure 2). Thus, there is a general tendency for more daily wind, precipitation, cold and hot ex-
168 tremes when the jet is regionally wavy. Locally, though, the opposite may be the case; for ex-
169 ample the odds of winter cold extremes over western Canada and Alaska are decreased when
170 the jet is wavy in the North American sector (see Figures 1 and 3, Supporting Figure 3 and
171 discussion in Section 3.3).

172 Carrying out the same analysis for hemispheric jet waviness shows that for both high
173 and low waviness, the land area of significant ORs is smaller for hemispheric than regional-
174 scale jet waviness (Figure 1, Supporting Figure 2). Hence, daily weather extremes are affected
175 primarily by regional-scale rather than hemispheric jet waviness. We next study the link be-
176 tween regional-scale jet waviness and extremes in more detail to show why the link is stronger
177 on regional scales and which flow configurations and synoptic weather patterns contribute to
178 the extremes.

179 **3.2 Precipitation and Wind Extremes**

180 We start with the ORs of winter (December-February, DJF) precipitation and wind ex-
181 tremes for high waviness in the North Atlantic sector (Figure 2(a,b)). A wavy North Atlantic
182 jet is associated with more frequent precipitation and wind extremes over northeastern Canada,
183 Greenland and off the coast of Morocco (odds increased by 50-150%), while over the British
184 Isles and parts of western Europe precipitation and wind extremes are less frequent (odds re-
185 duced by up to 75%). Moreover, a wavy North Atlantic jet is associated with more cyclones
186 between Newfoundland and Greenland and off the coast of Morocco, as well as a reduced cy-
187 clone frequency in the northeastern North Atlantic (Figure 2(a,b)).

188 The modulation of the cyclone frequencies explains the spatial patterns of the wind and
189 precipitation extreme ORs: as expected from prior knowledge, wind and precipitation extremes
190 are more frequent in areas with more cyclones. This is further illustrated for two grid points
191 located in the areas of high OR over the Davis Strait at $57^{\circ}\text{W}/62^{\circ}\text{N}$ and over the eastern sub-
192 tropical Atlantic at $15^{\circ}\text{W}/32^{\circ}\text{N}$ (Figure 2(c,d)). Precipitation extremes over the Davis Strait
193 during winter are associated with a cyclonically overturning dynamical tropopause, i.e. cyclonic
194 Rossby wave breaking, over the western North Atlantic, which produces the high waviness sig-
195 nal (Figure 2(c)). More frequent extratropical cyclones over Baffin Island and very high amounts
196 of moisture favor the occurrence of precipitation extremes (Figure 2(c)). The synoptic situ-
197 ation for wind extremes over the Davis Strait is similar (Supporting Figure S4). Precipitation

198 extremes over the subtropical eastern Atlantic occur during anticyclonic Rossby wave break-
199 ing events over the subtropical Atlantic (Figure 2(d)) and are associated with an enhanced cy-
200 clone frequency as well as increased atmospheric moisture content in the area of the precip-
201 itation extremes. These two composites illustrate a pivotal difficulty that arises when study-
202 ing the link between jet waviness and weather extremes: The high waviness days contain sev-
203 eral distinct synoptic flow configurations, even for relatively small longitudinal sectors, and
204 extremes in different areas of significant ORs do not necessarily occur on the same day. The
205 statistical analyses only pick up the most dominant of these flow configurations. Considering
206 hemispheric waviness thus leads to a strong "smoothing" of the synoptic link to the extremes
207 and hence less statistically significant ORs.

208 Results for other sectors and seasons further emphasize the key role of weather systems
209 in linking jet waviness to precipitation and wind extremes. For North Pacific jet waviness, OR
210 patterns are qualitatively similar to those for the North Atlantic (Supporting Figure 5). For high
211 Eurasian jet waviness significant ORs of wind and precipitation extremes are confined to the
212 Asian high Arctic (Supporting Figure 6), where these extremes are favored by high jet wavi-
213 ness. In regions where extratropical cyclones occur less frequently (Supporting Figure 1) ORs
214 of wind and precipitation extremes for high Eurasian jet waviness are similar to climatology
215 (Supporting Figure 6). During the summer months (July-August, JJA) OR patterns for wind
216 and precipitation extremes are qualitatively similar to winter (Supporting Figure 7), however,
217 the signals are weaker, conceivably due to the reduced number and intensity of extratropical
218 cyclones [Wernli and Schwerz, 2006] and more extremes occurring in association with smaller
219 scale processes such as convection.

220 **3.3 Cold Extremes**

221 We next look at cold extremes during DJF in the Atlantic sector (Figure 3(a)). A wavy
222 North Atlantic jet is associated with more frequent blocking situations over the central North
223 Atlantic and an increased number of cold extremes downstream in western Europe and parts
224 of the Mediterranean (Figure 3(a)). During days when cold extremes in western France at $4^{\circ}\text{W}/48^{\circ}\text{N}$
225 co-occur with high North Atlantic waviness, the blocking frequency is increased over the North
226 Atlantic and easterly and northeasterly winds advect cold air to western Europe (i.e., to the
227 south and downstream of the blocks, Figure 3(d)). This is in good agreement with previous
228 results of *Sillmann et al.* [2011] and *Buehler et al.* [2011]. There is also an area of significant
229 ORs in the subtropical Atlantic. Cold extremes in this region are related to an anticyclonic over-

230 turning of the tropopause over the subtropical Atlantic with a trough reaching far southward
231 bringing the cold air into the subtropics (Figure 3(c)). This flow configuration is accompanied
232 by an anomalously high blocking frequency upstream and to the north, over the western At-
233 lantic. Again cold extremes over the subtropical Atlantic and western Europe are linked to dis-
234 tinctly different, but all high waviness, upper-level flow configurations over the Atlantic.

235 Furthermore, a wavy jet over North America is associated with less frequent cold ex-
236 tremes over vast areas of western Canada and Alaska, as well as more frequent blocking over
237 central Canada (Figure 3(b)). Hence, these reduced odds conceivably result from more frequent
238 warm air advection and suppressed cold air advection in the western part of the blocks (see
239 also Supporting Figure 3).

240 **3.4 Hot Extremes**

241 Recent studies have suggested that changes in summer circulation might contribute sig-
242 nificantly to a further increase in the number of hot extremes [Francis and Vavrus, 2012, 2015;
243 Horton *et al.*, 2015; Coumou *et al.*, 2015], the hypothesis being that a more wavy jet stream
244 is associated with more frequent atmospheric blocks [Francis and Vavrus, 2012; Liu *et al.*, 2012;
245 Francis and Vavrus, 2015], which are conducive to summer hot extremes [Black *et al.*, 2004;
246 Barriopedro *et al.*, 2011; Pfahl and Wernli, 2012b; Horton *et al.*, 2015].

247 Indeed, a regionally wavy jet over the Northern Hemisphere land masses favors the oc-
248 currence of hot extremes (Figure 4). Over western Russia, for example, in the region where
249 the Russian heat wave in 2010 was most pronounced [Barriopedro *et al.*, 2011], the odds of
250 summer hot extremes are increased by up to 150% during days with a wavy Eurasian jet (Fig-
251 ure 4(a)). In the same area, the frequency of atmospheric blocking is increased by roughly 50%
252 compared to climatology (Figure 4(a) and Supporting Figure 1). A similar link is evident over
253 eastern Siberia and over North America, (Figure 4(a) and (b)), where a wavy jet in summer
254 favors more atmospheric blocking over Canada and is associated with more frequent hot ex-
255 tremes south of the Baffin Bay. Over the oceans, however, the ORs of summer hot extremes
256 do not differ significantly from climatology during days with high regional-scale jet waviness
257 (Supporting Figure 8), which is consistent with the findings of Pfahl and Wernli [2012b], as
258 discussed in Section 1.

4 Summary and Conclusions

This study reveals a statistically highly significant and meteorologically explicable link between regional-scale jet waviness and the occurrence of different types of daily mid-latitude weather extremes. Regional-scale jet waviness affects daily weather extremes through its linkage to synoptic-scale weather systems (cyclones and blocking) that trigger the extremes. In winter, the link between jet waviness and the occurrence of daily wind, precipitation and cold extremes is strongest in and around the Northern Hemisphere storm tracks, where these extremes occur mostly in association with synoptic-scale weather systems. Further away from the storm tracks, the odds of daily wind, precipitation and cold extremes are not significantly affected by regional-scale jet waviness. In summer, the waviness-extremes linkage weakens for wind and precipitation extremes, however, high jet waviness over the continents strongly enhances the number of hot extremes by favoring the occurrence of atmospheric blocking.

While the presented results are consistent with previous findings on the role of weather systems in triggering extremes, they also clearly show that the strength and sign of the waviness-extremes link varies depending on sector, season and type of extreme. This implies that if jet waviness is to change in regionally differing ways [Francis and Vavrus, 2012; Screen and Simmonds, 2013a; Francis and Vavrus, 2015; Francis and Skific, 2015], the implications for the occurrence of extremes will fundamentally depend on where jet waviness changes occur.

Compared to previous studies that investigated the linkage of weather extremes to hemispheric jet waviness [Liu *et al.*, 2012; Petoukhov *et al.*, 2013; Coumou *et al.*, 2014; Screen and Simmonds, 2014], the regional-scale waviness measure used here, enables clearer and more significant associations with weather extremes. In addition, the meteorological mechanisms responsible for this linkage are shown by incorporating changes in the frequency of synoptic-scale weather systems. Our findings have the following important implications for the discussion of altered weather extremes due to changes in jet waviness.

1. The link between jet waviness and the occurrence of weather extremes is stronger for regional-scale than hemispheric jet waviness and also varies between regions. Hence, waviness changes on regional scales are more relevant for changes in the frequency of weather extremes than changes in hemispheric jet waviness. Therefore, potential changes in jet waviness need to be identified regionally.
2. Jet waviness is linked to the occurrence of daily weather extremes via synoptic-scale weather systems. To understand future changes in the occurrence of daily weather ex-

291 tremes in the mid-latitudes, future research needs to assess how climate change affects
292 the number, intensity and pathway of synoptic-scale weather systems as well as their
293 ability to trigger extremes.

294 **Acknowledgments**

295 The authors thank the ECMWF for providing access to the ERA-Interim data, R. Beerli (ETH
296 Zürich) for helpful discussions about hypothesis testing and two reviewers which helped greatly
297 to improve the clarity of this manuscript. M.R. wishes to acknowledge the Swiss National Sci-
298 ence foundation for its financial support (Grant number 200021_159905/1). ERA-Interim data
299 can be accessed under <http://apps.ecmwf.int/datasets/data/interim-full-daily>.

300 **References**

- 301 Barnes, E. A. (2013), Revisiting the evidence linking Arctic amplification to extreme
302 weather in midlatitudes, *Geophys. Res. Lett.*, *40*, 4734–4739, doi:10.1002/grl.50880.
- 303 Barnes, E. A., and J. A. Screen (2015), The impact of Arctic warming on the midlatitude
304 jet-stream: Can it? Has it? Will it?, *Wiley Interdiscip. Rev. Clim. Chang.*, *6*, 277–286,
305 doi:10.1002/wcc.337.
- 306 Barriopedro, D., E. M. Fischer, J. Luterbacher, R. M. Trigo, and R. García-Herrera (2011),
307 The hot summer of 2010: redrawing the temperature record map of Europe, *Science*,
308 *332*, 220–224, doi:10.1126/science.1201224.
- 309 Benjamini, Y., and Y. Hochberg (1995), Controlling the false discovery rate: a practical
310 and powerful approach to multiple testing, *J. Roy. Stat. Soc. B Met.*, *57*, 289–300.
- 311 Black, E., M. Blackburn, G. Harrison, B. Hoskins, and J. Methven (2004), Factors
312 contributing to the summer 2003 European heatwave, *Weather*, *59*, 217–223, doi:
313 10.1256/wea.74.04.
- 314 Buehler, T., C. C. Raible, and T. F. Stocker (2011), The relationship of winter season
315 North Atlantic blocking frequencies to extreme cold or dry spells in the ERA-40, *Tellus*
316 *A*, *63*, 212–222, doi:10.1111/j.1600-0870.2010.00492.x.
- 317 Coumou, D., and S. Rahmstorf (2012), A decade of weather extremes, *Nat. Clim. Change*,
318 *2*, 491–496, doi:10.1038/nclimate1452.
- 319 Coumou, D., V. Petoukhov, S. Rahmstorf, S. Petri, and H. J. Schellnhuber (2014),
320 Quasi-resonant circulation regimes and hemispheric synchronization of extreme
321 weather in boreal summer, *P. Natl. Acad. Sci. USA*, *111*, 12,331–12,336, doi:

322 10.1073/pnas.1412797111.

323 Coumou, D., J. Lehmann, and J. Beckmann (2015), The weakening summer cir-
324 culation in the Northern Hemisphere mid-latitudes, *Science*, *348*, 324–327, doi:
325 10.1126/science.1261768.

326 Davies, H. C. (2015), Weather chains during the 2013/2014 winter and their significance
327 for seasonal prediction, *Nat. Geosci.*, *8*, 833837, doi:10.1038/ngeo2561.

328 Dee, D. P., S. M. Uppala, A. J. Simmons, P. Berrisford, P. Poli, S. Kobayashi, U. Andrae,
329 M. A. Balmaseda, G. Balsamo, P. Bauer, P. Bechtold, A. C. M. Beljaars, L. van de
330 Berg, J. Bidlot, N. Bormann, C. Delsol, R. Dragani, M. Fuentes, A. J. Geer, L. Haim-
331 berger, S. B. Healy, H. Hersbach, E. V. Hólm, L. Isaksen, P. Kallberg, M. Köhler,
332 M. Matricardi, A. P. McNally, B. M. Monge-Sanz, J. J. Morcrette, B. K. Park,
333 C. Peubey, P. de Rosnay, C. Tavolato, J. N. Thépaut, and F. Vitart (2011), The ERA-
334 Interim reanalysis: Configuration and performance of the data assimilation system, *Q. J.*
335 *Roy. Meteor. Soc.*, *137*, 553–597, doi:10.1002/qj.828.

336 Dickson, R. R., and J. Namias (1976), North American influences on the circulation and
337 climate of the North Atlantic sector, *Mon. Weather Rev.*, *104*(10), 1255–1265, doi:
338 10.1175/1520-0493(1976)104<1255:NAIOTC>2.0.CO;2.

339 Donat, M. G., G. C. Leckebusch, J. G. Pinto, and U. Ulbrich (2010), Examination of wind
340 storms over Central Europe with respect to circulation weather types and NAO phases,
341 *Int. J. Climatol.*, *30*(9), 1289–1300, doi:10.1002/joc.1982.

342 Fischer, E. M., S. Seneviratne, P. Vidale, D. Lüthi, and C. Schär (2007), Soil moisture-
343 atmosphere interactions during the 2003 European summer heat wave, *J. Climate*,
344 *20*(20), 5081–5099, doi:10.1175/JCLI4288.1.

345 Francis, J., and N. Skific (2015), Evidence linking rapid Arctic warming to mid-latitude
346 weather patterns, *Phil. Trans. R. Soc. A*, *373*, 20140,170, doi:0.1098/rsta.2014.0170.

347 Francis, J. A., and S. J. Vavrus (2012), Evidence linking Arctic amplification to extreme
348 weather in mid-latitudes, *Geophys. Res. Lett.*, *39*(6), doi:10.1029/2012GL051000.

349 Francis, J. A., and S. J. Vavrus (2015), Evidence for a wavier jet stream in response to
350 rapid Arctic warming, *Environ. Res. Lett.*, *10*(1), doi:10.1088/1748-9326/10/1/014005.

351 Herring, S. C., M. P. Hoerling, T. C. Peterson, and P. A. Stott (2014), Explaining extreme
352 events of 2013 from a climate perspective, *Bull. Amer. Meteorol. Soc.*, *95*, S1–S104,
353 doi:10.1175/1520-0477-95.9.S1.1.

- 354 Horton, D. E., N. C. Johnson, D. Singh, D. L. Swain, B. Rajaratnam, and N. S. Diffen-
355 baugh (2015), Contribution of changes in atmospheric circulation patterns to extreme
356 temperature trends, *Nature*, 522, 465–469, doi:10.1038/nature14550.
- 357 Hoskins, B. J., and T. Woollings (2015), Persistent extratropical regimes and climate ex-
358 tremes, *Current Climate Change Reports*, 1, 115–124, doi:10.1007/s40641-015-0020-8.
- 359 IPCC (2012), *Managing the Risks of Extreme Events and Disasters to Advance Climate*
360 *Change Adaptation. A Special Report of Working Groups I and II of the Intergovernmental*
361 *Panel on Climate Change*, 582 pp., Cambridge University Press.
- 362 Lehmann, J., and D. Coumou (2015), The influence of mid-latitude storm tracks on hot,
363 cold, dry and wet extremes, *Sci. Rep.*, 5(17491), doi:10.1038/srep17491.
- 364 Liu, J., J. A. Curry, H. Wang, M. Song, and R. M. Horton (2012), Impact of declining
365 Arctic sea ice on winter snowfall, *Proc. Natl. Acad. Sci. USA*, 109, 4074–4079, doi:
366 10.1073/pnas.1114910109.
- 367 Martius, O., C. Schwierz, and H. C. Davies (2010), Tropopause-level waveguides, *J.*
368 *Atmos. Sci.*, 67, 866–879, doi:10.1175/2009JAS2995.1.
- 369 Namias, J. (1960), Factors in the initiation, perpetuation and termination of drought, *Inter-*
370 *national Association of Scientific Hydrology Commission on Surface Waters Publication*,
371 51, 81–94.
- 372 Palmer, T. (2014), Record-breaking winters and global climate change, *Science*, 344,
373 803–804, doi:10.1126/science.1255147.
- 374 Petoukhov, V., S. Rahmstorf, S. Petri, and H. J. Schellnhuber (2013), Quasiresonant ampli-
375 fication of planetary waves and recent Northern Hemisphere weather extremes, *P. Natl.*
376 *Acad. Sci. USA*, 110, 5336–5341, doi:10.1073/pnas.1222000110.
- 377 Pfahl, S., and H. Wernli (2012a), Quantifying the relevance of cyclones for precipitation
378 extremes, *J. Climate*, 25, 6770–6780, doi:10.1175/JCLI-D-11-00705.1.
- 379 Pfahl, S., and H. Wernli (2012b), Quantifying the relevance of atmospheric blocking
380 for co-located temperature extremes in the Northern Hemisphere on (sub-) daily time
381 scales, *Geophys. Res. Lett.*, 39(12), doi:10.1029/2012GL052261.
- 382 Röthlisberger, M., O. Martius, and H. Wernli (2016), An algorithm for identifying the
383 initiation of synoptic-scale Rossby waves on potential vorticity waveguides, *Q. J. Roy.*
384 *Meteor. Soc.*, 142(695), 889–900, doi:10.1002/qj.2690.
- 385 Schneider, T., T. Bischoff, and H. Płotka (2015), Physics of changes in synoptic mid-
386 latitude temperature variability, *J. Climate*, 28, 2312–2331, doi:10.1175/JCLI-D-14-

387 00632.1.

388 Schwierz, C., M. Croci-Maspoli, and H. Davies (2004), Perspicacious indicators of atmo-
389 spheric blocking, *Geophys. Res. Lett.*, *31*(6), doi:10.1029/2003GL019341.

390 Screen, J. A., and I. Simmonds (2013a), Exploring links between Arctic amplification and
391 mid-latitude weather, *Geophys. Res. Lett.*, *40*, 959–964, doi:10.1002/grl.50174.

392 Screen, J. A., and I. Simmonds (2013b), Caution needed when linking weather extremes
393 to amplified planetary waves, *Proceedings of the National Academy of Sciences*, *110*(26),
394 E2327–E2327, doi:10.1073/pnas.1304867110.

395 Screen, J. A., and I. Simmonds (2014), Amplified mid-latitude planetary waves
396 favour particular regional weather extremes, *Nat. Clim. Change*, *4*, 704–709, doi:
397 10.1038/nclimate2271.

398 Seneviratne, S. I., T. Corti, E. L. Davin, M. Hirschi, E. B. Jaeger, I. Lehner, B. Or-
399 lowskey, and A. J. Teuling (2010), Investigating soil moisture–climate interactions
400 in a changing climate: A review, *Earth-Science Reviews*, *99*(3), 125–161, doi:
401 10.1016/j.earscirev.2010.02.004.

402 Sillmann, J., M. Croci-Maspoli, M. Kallache, and R. W. Katz (2011), Extreme cold winter
403 temperatures in Europe under the influence of North Atlantic atmospheric blocking, *J.*
404 *Climate*, *24*, 5899–5913, doi:10.1175/2011JCLI4075.1.

405 Stephenson, D. B. (2000), Use of the odds ratio for diagnosing forecast skill, *Weather*
406 *Forecast.*, *15*(2), 221–232, doi:10.1175/1520-0434(2000)015;0221:UOTORF₂.0.CO;2.

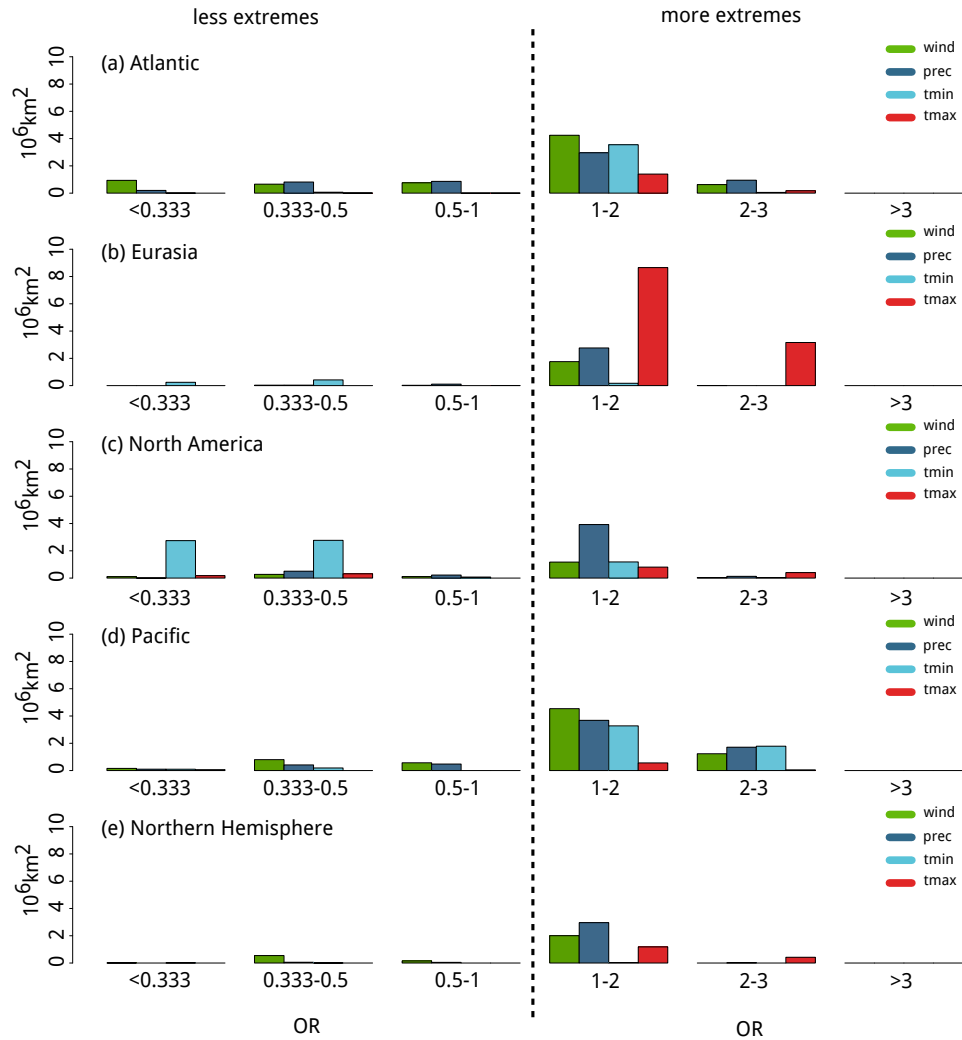
407 Ventura, V., C. J. Paciorek, and J. S. Risbey (2004), Controlling the proportion of falsely
408 rejected hypotheses when conducting multiple tests with climatological data, *J. Climate*,
409 *17*, 4343–4356, doi:10.1175/3199.1.

410 Vose, R. S., S. Applequist, M. A. Bourassa, S. C. Pryor, R. J. Barthelmie, B. Blanton,
411 P. D. Bromirski, H. E. Brooks, A. T. DeGaetano, R. M. Dole, et al. (2014), Monitoring
412 and understanding changes in extremes: Extratropical storms, winds, and waves, *Bull.*
413 *Amer. Meteorol. Soc.*, *95*, 377–386, doi:10.1175/BAMS-D-12-00162.1.

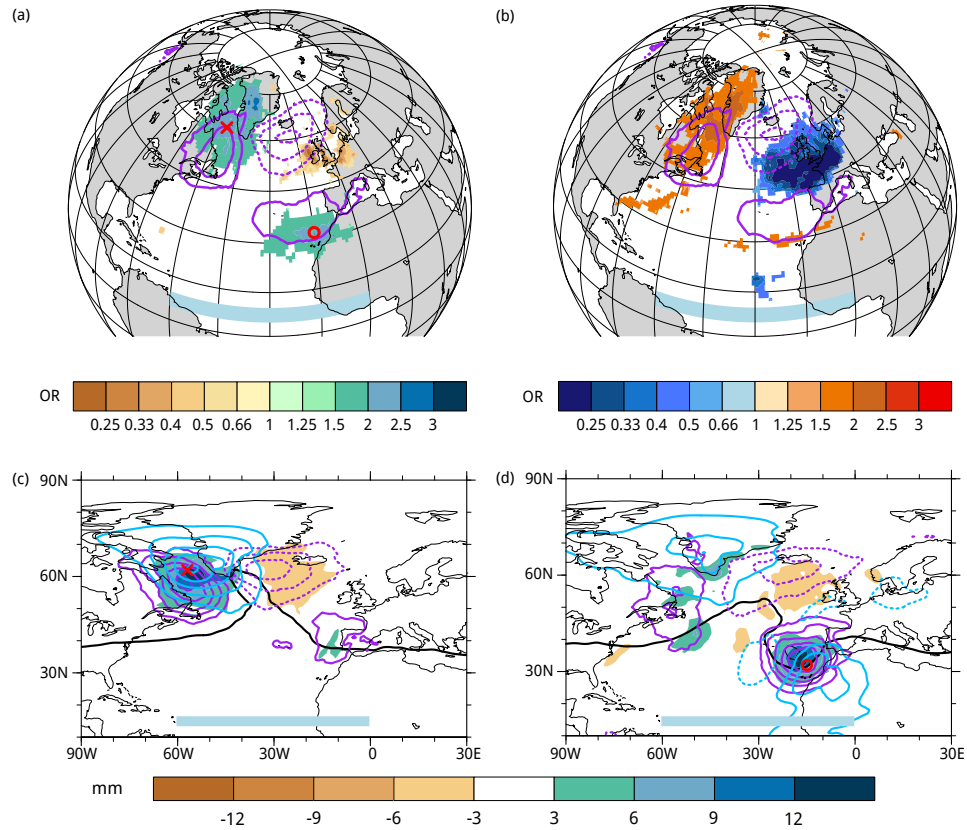
414 Wernli, H., and C. Schwierz (2006), Surface cyclones in the ERA40 data set (1958–2001).
415 Part I: Novel identification method and global climatology, *J. Atmos. Sci.*, *63*, 2486–
416 2507, doi:10.1175/JAS3766.1.

417 Whan, K., F. Zwiers, and J. Sillmann (2016), The influence of atmospheric blocking
418 on extreme winter minimum temperatures in north america, *J. Climate*, (2016), doi:
419 10.1175/JCLI-D-15-0493.1.

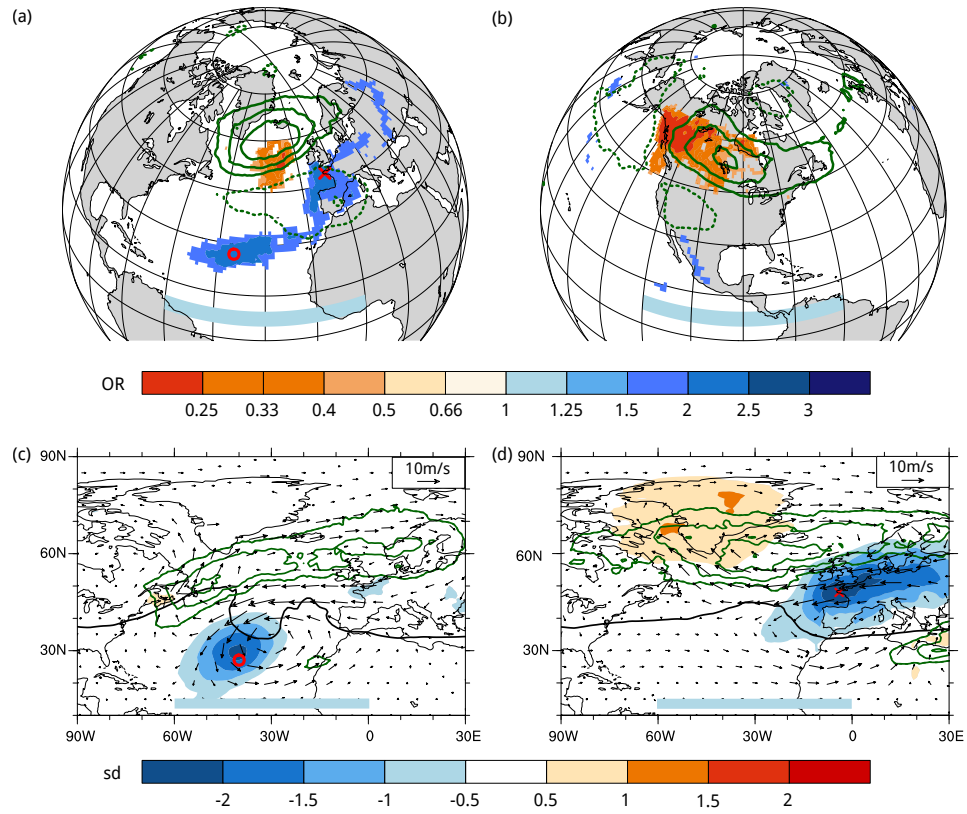
420 Wilks, D. S. (2011), *Statistical Methods in the Atmospheric Sciences, International Geo-*
421 *physics Series*, vol. 100, 3 ed., Elsevier Inc, doi:10.1016/B978-0-12-385022-5.00001-4.



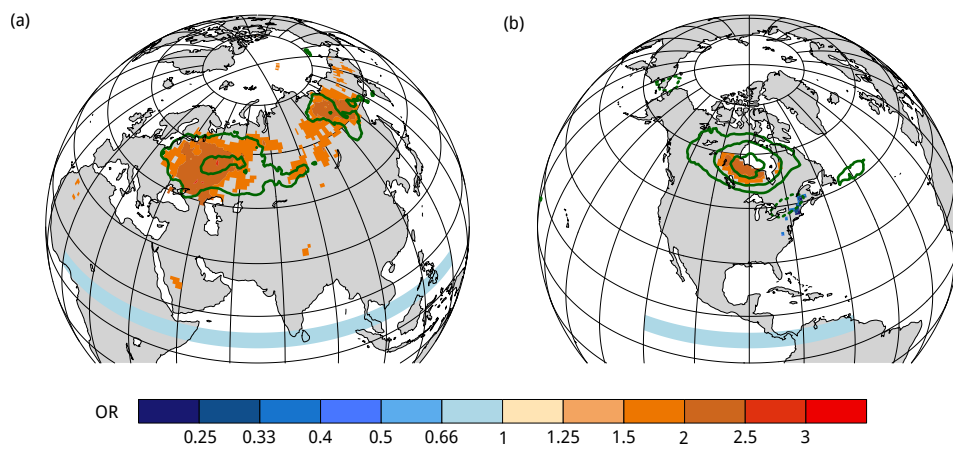
422 **Figure 1.** Land area north of 10°N with statistically significant ORs of DJF wind (green), DJF precipi-
 423 tation (dark blue), DJF cold (light blue) and JJA hot (red) extremes for high waviness in the North Atlantic
 424 (a), the Eurasian (b), the North American (c) and the North Pacific (d) sector and in the entire Northern
 425 Hemisphere (e) for different OR categories.



426 **Figure 2.** Statistically significant ORs of (a) precipitation and (b) wind gust extremes for high waviness
 427 in the North Atlantic sector (indicated with light blue bars). Solid (dashed) purple contours depict positive
 428 (negative) cyclone frequency anomalies for DJF high waviness days in the Atlantic sector in absolute per-
 429 centage points starting from 5pp (-5pp), every 5pp (-5pp). Panels (c) and (d) depict composites of various
 430 variables for days when high waviness in the North Atlantic sector co-occurs with a precipitation extreme
 431 at 57°W/62°N (c) and at 15°W/32°N (d): Precipitation anomaly relative to the DJF daily mean precipita-
 432 tion (shading), cyclone frequency anomaly as in (a,b) but starting from 10pp every 10pp, composite 2 PVU
 433 contour (solid black) and standardized anomalies of the vertically integrated specific humidity in light blue,
 434 starting at plus (solid) and minus (dashed) 0.5 standard deviation, every 0.5 standard deviation. Red crosses
 435 and circles indicate the two grid points.



436 **Figure 3.** Statistically significant ORs of DJF cold extremes for high waviness in the (a) Atlantic and (b)
 437 North American sector (sectors indicated with light blue bars in all panels). Solid (dashed) green contours
 438 depict positive (negative) blocking frequency anomalies for DJF high waviness days in the respective sector in
 439 absolute percentage points starting from 5pp (-5pp), every 5pp (-5pp). Panels (c) and (d) depict composites of
 440 various variables for days when high waviness in the North Atlantic sector co-occurs with a precipitation ex-
 441 tremre at 40°W/27°N (c) and at 4°W/40°N (d): Standardized 2 m temperature anomaly (shading), blocking
 442 frequency anomaly as in (a,b) but starting from 10pp every 10pp, composite 2 PVU contour (solid black) and
 443 wind anomalies at 850 hPa. Red crosses and circles indicate the two grid points.



444 **Figure 4.** Statistically significant ORs of JJA hot extremes for high jet waviness in the (a) Eurasian sector
445 and (b) the North American sector. Green contours (blocking frequency anomaly) as in Figure 3. The blue bar
446 depicts the extent of the respective sector.